Supplementary Information for

The 8.2k event: abrupt transition of the subpolar gyre towards a modern North Atlantic circulation

Andreas Born[1]

Bjerknes Centre for Climate Research, Bergen, Norway

Geophysical Institute, University of Bergen, Bergen, Norway

Anders Levermann

Potsdam Institute for Climate Impact Research, Potsdam, Germany

Institute of Physics, Potsdam University, Potsdam, Germany

This Supplement is organized as follows: The climate model is described in detail in section 1. Section 2 discusses the robustness of multiple subpolar gyre (SPG) modes by presenting findings from several climate models. Section 3 continues this discussion summarizing work on the sensitivity of the SPG primarily in CLIM*BER*-3α. This is followed by figures supporting conclusions in the main text and a table referencing the marine sediment cores discussed in the main text in section 4.

[1] Corresponding author: andreas.born@bjerknes.uib.no

1 The climate model CLIM*BER*-3α and experimental design

CLIM*BER*-3α consists of the statistical-dynamical atmosphere model POTSDAM-2 (*Petoukhov et al.*, 2000) coupled to a global ocean general circulation model based on the Geophysical Fluid Dynamics Laboratory (GFDL) Modular Ocean Model (MOM-3) code and to the dynamic and thermodynamic sea ice module of *Fichefet and Maqueda* (1997). The oceanic horizontal resolution is 3.75° × 3.75° with 24 unevenly spaced vertical layers. We apply a weak background vertical diffusivity of $0.2 \times 10^{-4} m^2 s^{-1}$. For a discussion on the model's sensitivity to this parameter refer to *Mignot et al.* (2006). The implemented second-order moment tracer advection scheme (*Prather*, 1986) minimizes numerical diffusion (*Hofmann and Maqueda*, 2006). The model makes use of a parametrization of boundary enhanced mixing depending both on near-bottom stratification and roughness of topography (*Ledwell et al.*, 2000), following *Hasumi and Suginohara* (1999). This leads locally to vertical diffusion coefficients of up to $10^{-4} m^2 s^{-1}$ for example over rough topography.

The atmosphere model has a coarse spatial resolution (7.5° in latitude and 22.5° in longitude) and is based on the assumption of a universal vertical structure of temperature and humidity, which allows reducing the three-dimensional description to a set of two-dimensional prognostic equations. Description of atmospheric dynamics is based on a quasi-geostrophic approach and a parametrization of the zonally averaged meridional atmospheric circulation. Synoptic processes are parametrized as diffusion terms with a turbulent diffusivity computed from atmospheric stability and horizontal temperature gradients. Heat and freshwater fluxes between ocean and atmosphere are computed on the oceanic grid and applied without any flux adjustments. The wind stress is computed as the sum of the NCEP-NCAR reanalysis wind stress climatology (*Kalnay and coauthors*, 1996) and the wind stress anomaly calculated by the atmospheric model relative to the control run. CLIM*BER*-3α has been validated against data both for Holocene (*Montoya et al.*, 2005) and glacial boundary conditions (*Montoya and Levermann*, 2008).

Deep water formation takes place in two regions, north of the Greenland Scotland ridge and in the SPG center. Deep water masses are communicated by overflows

through the deepest passages of the ridge. This deep outflow from the Nordic Seas facilitates a surface inflow in our model. Although only crudely represented, the exchange shows the dynamical behavior expected from Holocene paleo data (*Solignac et al.*, 2004) and model studies (*Renssen et al.*, 2005). In CLIM*BER*-3α, salinity gradients in the subpolar region are generally sharper than in fields provided by *Levitus* (1982) (compare *Montoya et al.* (2005)). Since these climatological reconstructions have a general tendency towards less pronounced density gradients compared to direct observations this feature is not necessarily unrealistic.

2 Evidence for multiple subpolar gyre modes in other models

The positive feedbacks that give rise to the SPG bistability are based exclusively on large scale dynamics. Thus, they are likely to be found in most ocean models even though the existence of multiple stable SPG modes circulation might be masked by other processes. While there are good indications from proxy data that a transition between two SPG modes took place indeed and was not masked by such secondary processes, here we shortly present some fundamental considerations regarding the existence of positive SPG feedbacks and discuss indications for these feedbacks in a number of different ocean models.

Convection in the SPG center is intimately linked to its strength (*Eden and Willebrand*, 2001; *Häkkinen and Rhines*, 2004; *Treguier et al.*, 2005; *Born et al.*, 2010a), because it increases density in the gyre's center around which water circulates baroclinically (*Born et al.*, 2009). Thus the bistability of the SPG circulation can also be understood in the framework of convection, with stronger convection entailing a stronger gyre. In addition, a stronger SPG advects more saline water into the western North Atlantic facilitating convection, a positive feedback that destabilizes the system (*Levermann and Born*, 2007).

Different modes of Labrador Sea deep convection are found in many ocean models. In HadCM3, *Kleinen et al.* (2009) discuss a 70 % weakening of the SPG coeval with a reduction of Labrador Sea convection in response to continuous freshwater forcing

of the North Atlantic. Experiments with anomalous heat transports over Labrador Sea by *Wu and Wood* (2008) exhibit an abrupt strengthening of the SPG for higher heat loss and convection. A weaker SPG circulation in response to weaker convection in its center has also been confirmed for the Institut Pierre Simon Laplace Coupled Model 4 (IPSL CM4) (*Born et al.*, 2010a). The positive feedback related to a weaker salt transport by the SPG was also quantified in this study.

In addition to *Levermann and Born* (2007), some further studies directly report on spontaneous transitions between active and inactive Labrador Sea convection modes. These suggest the presence of destabilizing positive feedbacks. *Jongma et al.* (2007) discuss a bistability of convection and overturning circulation. Their model (ECBilt-Clio) alternates between two meta-stable states with active and inactive convection. Along with an externally applied constant freshwater perturbation over Labrador Sea, the residence time in the inactive convection state gradually increases. *LeGrande et al.* (2006) and *LeGrande and Schmidt* (2008) also find a spontaneous transition to active Labrador Sea convection in their preindustrial control run with the Goddard Institute for Space Studies ModelE-R atmosphere ocean general circulation model. Two states of SPG circulation have also been observed in the Bergen Climate Model, an AOGCM (H. Drange, personal communication, 2009).

While models over a wide range of complexity suggest the existence of multiple SPG modes, earlier model simulations of the 8.2k event did not report persistent changes in the SPG circulation. Without the coeval intensification of deepwater formation south of the Greenland Scotland ridge, these models usually report a strong reduction of the Atlantic Meridional Overturning Circulation (AMOC), an apparent contradiction of our results. This is possibly due to the direct application of the meltwater pulse on the Labrador Sea convection region. As pointed out above, convection in the gyre's center has strong control on its strength, which will be discussed in more detail in the following section. *Bauer et al.* (2004) employ a zonally averaged, two-dimensional, ocean model. Hence, the freshwater anomaly is distributed over the entire basin width and inevitably affects convection south of the Greenland Scotland ridge directly. Moreover, gyre dynamics cannot be adequately included in zonally averaged models. *LeGrande et al.* (2006) and *LeGrande and Schmidt* (2008) simulate the 8.2k event in a three-dimensional ocean model using two different initial

states. One result is that the state more realistic for the early Holocene, with weak Labrador Sea convection, simulates a significantly weaker AMOC reduction (30 %) than the strong initial state (50 %). This supports our findings that it is important not to apply the meltwater pulse directly on the convection region. *Wiersma et al.* (2006) also report a weaker AMOC reduction when applying the meltwater pulse on a weak Labrador Sea convection state. However, in this study the meltwater pulse is applied in the center of the Labrador Sea and directly on the convection region, which is still active in the weak state. This forcing scenario favors a strong AMOC response but disagrees with paleo data (*Hillaire-Marcel et al.*, 2007; *Keigwin et al.*, 2005) and a high resolution model study (*Winsor et al.*, 2006). Another consequence of applying the meltwater pulse directly onto the Labrador Sea convection region is that it removes a significant fraction of the meltwater pulse from the surface. Hence, a smaller fraction is advected into the Nordic Seas. This, however, is crucial to initiate the mechanism amplifying the SPG as has been shown in the main text.

3 Model sensitivity of the subpolar gyre circulation to changes in external forcing

The strength of the SPG depends at least partially on the density gradient between its center and rim. The water column in the center is relatively denser, causing a depression in sea surface height around which water circulates cyclonically in geostrophic balance. Increasing this density gradient results in a deeper depression and a stronger gyre. This understanding differentiates two classes of mechanisms controlling the SPG strength, by modifying the density of the water column in its center or the rim (Fig. S1).

3.1 Sensitivity to the representation of Greenland Scotland ridge overflow and anomalous freshwater forcing

Density at the northern rim of the SPG is partially controlled by dense waters overflowing the Greenland Scotland ridge. Because the representation of these small scale

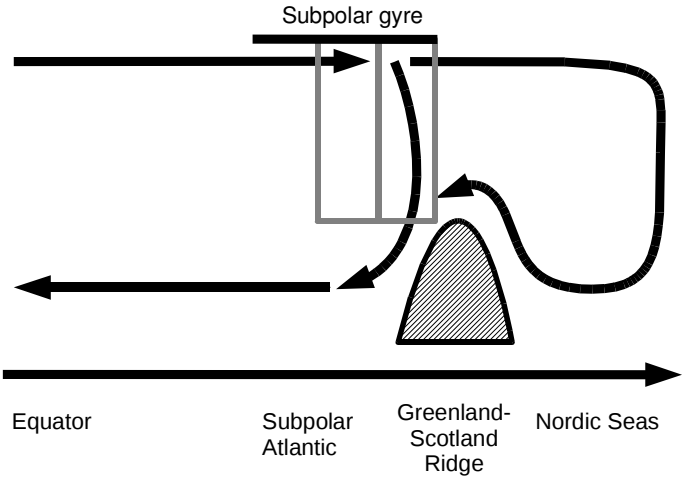

Figure S1: Schematic of the Atlantic Meridional Overturning Circulation (AMOC) and the subpolar gyre. Grey boxes show the center and exterior regions of the gyre referred to in the main text. Density changes in the center region are the result of positive feedbacks inherent to the subpolar gyre. The density on its rim is determined by two water masses mixing at intermediate depth, the denser one reaching the mixing region after sinking in the Nordic Seas and overflowing the Greenland-Scotland ridge and a second produced by sinking south of the ridge.

currents is essential for the formation of North Atlantic Deep Water but problematic in ocean general circulation models, it is often enhanced by means of numerical techniques. A study of two different approaches, namely artificial deepending of the ridge and a hydraulic overflow parametrization, found that both simulate the large scale deep ocean circulation similarly well. However, the density of the resulting water mass south of the Greenland Scotland ridge, thus at the SPG rim, is lower in one case resulting in a significantly stronger SPG (*Born et al.*, 2009).

Besides continuous changes in the overflow transport, we also investigated the sensitivity of the SPG to a transient reduction in overflow strength in response to anomalous freshwater flux into the Nordic Seas (*Levermann and Born*, 2007). Two main conclusions can be drawn from this study. First, the increase in SPG strength persists even after the freshwater pulse. This illustrates the relative importance of reduced overflows and density in the SPG rim on one side to positive feedbacks of the SPG that increase the density in the gyre's center on the other, while both mechanisms strengthen the circulation. Once the SPG reaches a critical strength

due to the overflows reduction, the SPG feedbacks increase the density in the SPG center and stabilize the strong circulation mode. Secondly, a freshwater pulse of 0.05 Sv over 25 years is sufficient to trigger a notable increase in SPG strength (Fig. S2). This is about a fourth of the lake Agassiz drainage volume and a good approximation to the fraction of the drainage that is advected into the Nordic Seas over a similar period of time ($\sim$ 30 years, Fig. 3 in the main text). This earlier sensitivity study strongly supports the simulation presented here for the 8.2k event.

The dilution of the lake drainage before reaching the main impact region, the Nordic Seas, the multi-decadal delay due to advection and the fact that a fraction of the original freshwater volume is enough to trigger the transition helps to assess the importance of a possible multipulse event of two smaller volume discharges as proposed from observations (*Ellison et al.*, 2006).

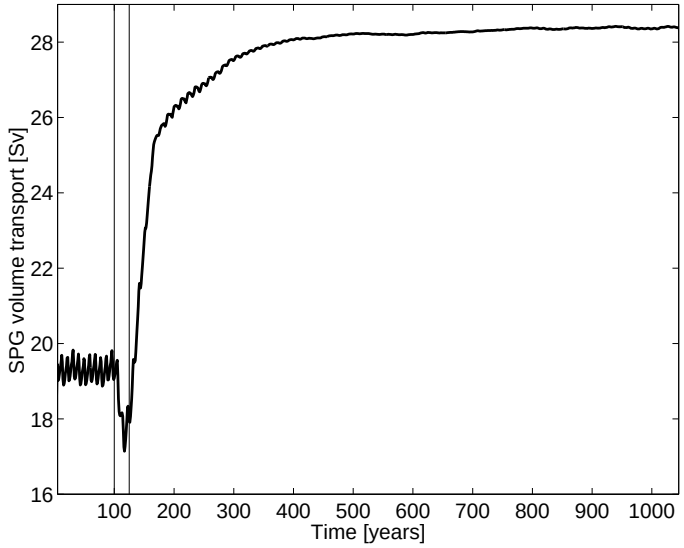

Figure S2: Temporal evolution of the SPG strength in response to freshwater forcing in the Nordic Seas. The vertical lines indicates the forcing period (25 years).

3.2 Sensitivity to wind stress

The transition of the SPG is robust to fixed surface wind stress (Fig. S3). In our model, the applied surface wind stress is generally based on anomalies from the

atmospheric model added to climatological averages. We repeated the experiment presented in *Levermann and Born* (2007) with surface wind stress prescribed to climatology in order to test the sensitivity of the SPG transition to this technique.

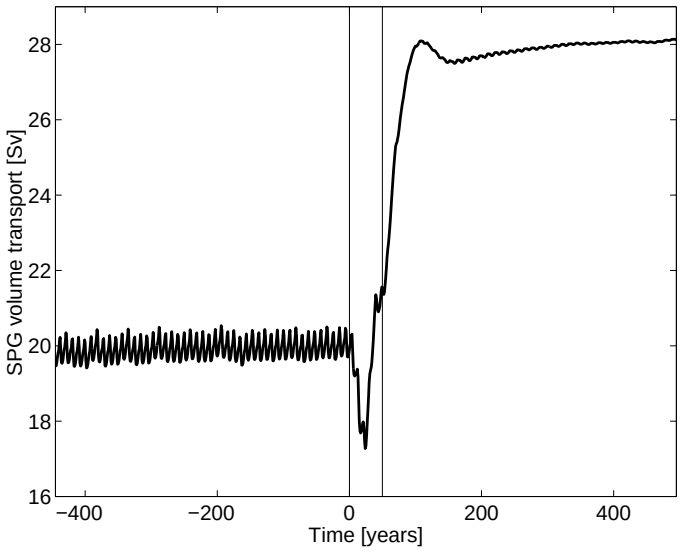

Figure S3: Temporal evolution of the SPG strength for an experiment with winds stress prescribed to present day climatology.

In addition, the sensitivity to scalar multiples of the climatological wind stress ranging over $\alpha \in [0.25, 2]$ has been investigated in preindustrial and Last Glacial Maximum (LGM) climate (*Montoya et al.*, 2010). The SPG strength is found to be considerably stronger in preindustrial than in LGM experiments, showing a qualitatively different sensitivity to surface wind stress. Under preindustrial boundary conditions, it decreases with increasing wind stress. Under LGM boundary conditions, it generally increases linearly with wind stress extrapolating to zero for zero wind stress. However, beyond a certain threshold for the wind stress the SPG sensitivity is reversed in the LGM and decreases with wind stress as well. This threshold is associated with the initiation of deep water formation in the Nordic Seas and the accompanying intensification of the Greenland Scotland ridge overflows.

Hence, even for changes in surface wind stress, the primary means of communicating this perturbation to the SPG is the overflow transport. This result from a fundamentally different set of experiments underlines the pivotal role of deep ocean

baroclinicity for the sensitivity of the SPG and supports the findings of the present study.

3.3 Sensitivity to vertical mixing

The bistability of the SPG is robust to changes in vertical diffusivity. Global background diffusivity in our model is $\kappa = 0.2 \times 10^{-4} m^2 s^{-1}$. However, experiments with $\kappa = 0.5 \times 10^{-4} m^2 s^{-1}$ also show two stable SPG modes and with even larger contrast in strength (Fig. S4).

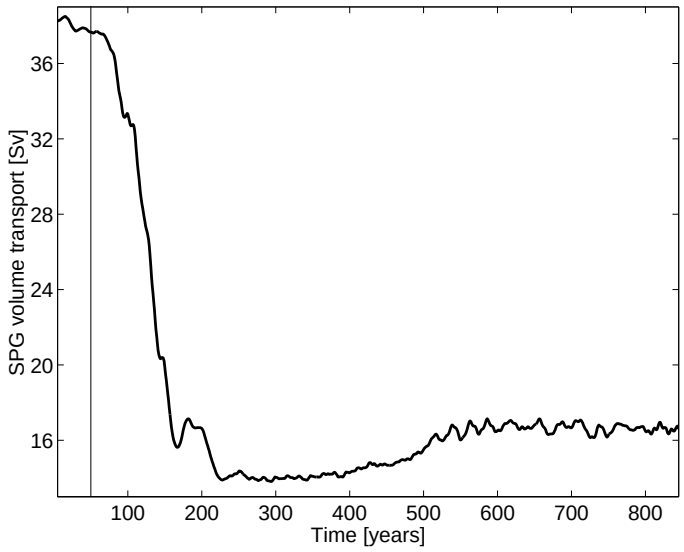

Figure S4: Temporal evolution of the SPG strength in a model version with higher vertical diffusivity. Starting from the strong circulation mode, a negative freshwater pulse of 0.1 Sv is applied over the first 50 years.

Multiple SPG equilibria are also found in a more fundamentally altered model set up. **?** implemented a stratification-dependent mixing scheme and forced the model with an 1%-per-year increase scenario of atmospheric CO_2. Warming and enhanced freshwater influx reduce the surface density of the North Atlantic as the CO_2 concentration increases. This results in stronger stratification, thus weaker vertical mixing and a density increase in subsurface water masses that feed the Greenland Scotland ridge. If the sensitivity of the mixing to stratification is raised

above a certain critical level, the weakening of the SPG is enhanced by the positive feedbacks described by *Levermann and Born* (2007).

3.4 Sensitivity to orbital parameters changes

The simulation of lake Agassiz drainage with preindustrial boundary conditions, i.e. with lower northern hemisphere summer insolation levels, gives a similar result (Fig. S5). This demonstrates the strength and robustness of the feedbacks involved.

However, with an even bigger change in orbital geometry one or the other circulation mode is preferred in CLIM*BER*-3α and IPSL CM4 (*Born et al.*, 2010a,b). A decrease in northern hemisphere summer insolation between 126,000 and 115,000 years before present is most pronounced in high northern latitudes. It thus favors Arctic sea ice growth causing an increase in sea ice export and a freshening south of Greenland. As a consequence, convection in the center of the SPG shuts down, density in the SPG center decreases and the gyre weakens. The analysis of the underlying dynamics confirm that the reorganization of the subpolar surface circulation is due to the same mechanism in both models indeed. However, changes in Arctic sea ice are much smaller for the simulated freshwater flood in this study and probably do not play a role for the stabilization of the circulation.

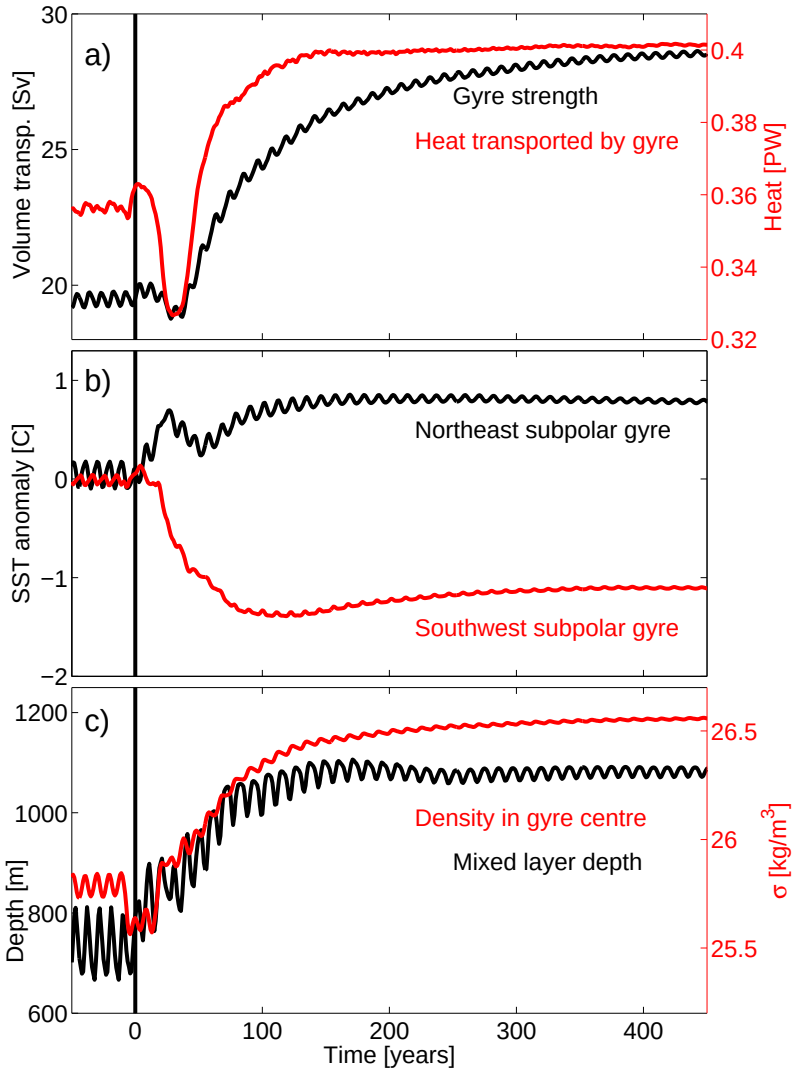

Figure S5: Simulation of the lake drainage in preindustrial climate, similar to figure 2 of the main text. The vertical line indicates the timing of the freshwater perturbation, data is filtered with a 25-year running mean. **a)** Volume and heat transport of the SPG; **b)** sea surface temperature in the north-eastern (black) and south-western (red) subpolar region; **c)** maximum winter mixed layer depth in the center of the SPG and surface density in the center of the SPG (see Fig. S7). The transition of the SPG and the underlying feedbacks are robust to a change in orbital geometry.

4 Supplemental figures and list of sediment cores

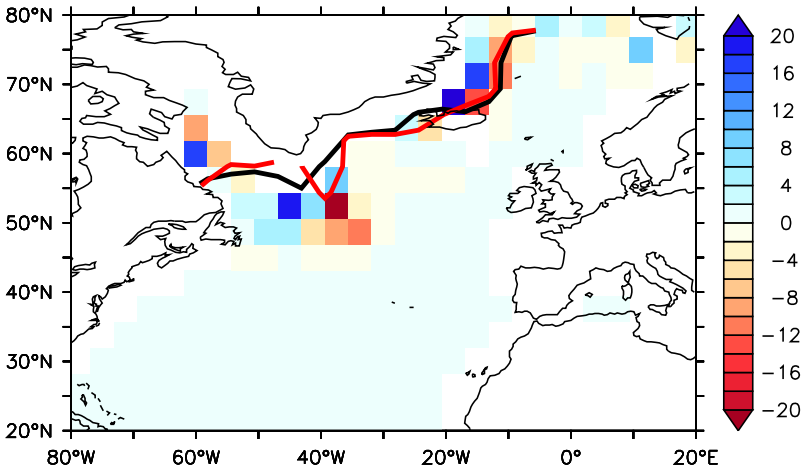

Figure S6: Colors: percental change in wind stress curl 'after' minus 'before' meltwater pulse; Contours: 15% sea ice concentration January to March average after (black) and before (red) transition. Wind stress curl changes are small, below 20% compared to the 47% strengthening of the SPG, and do not show a consistent pattern. Potential upwind changes in elevation, albedo or heat capacity due to the lake drainage are neglected in the model. Thus, the shown wind stress curl anomalies are likely due to local changes in sea ice as suggested also by the irregular pattern.

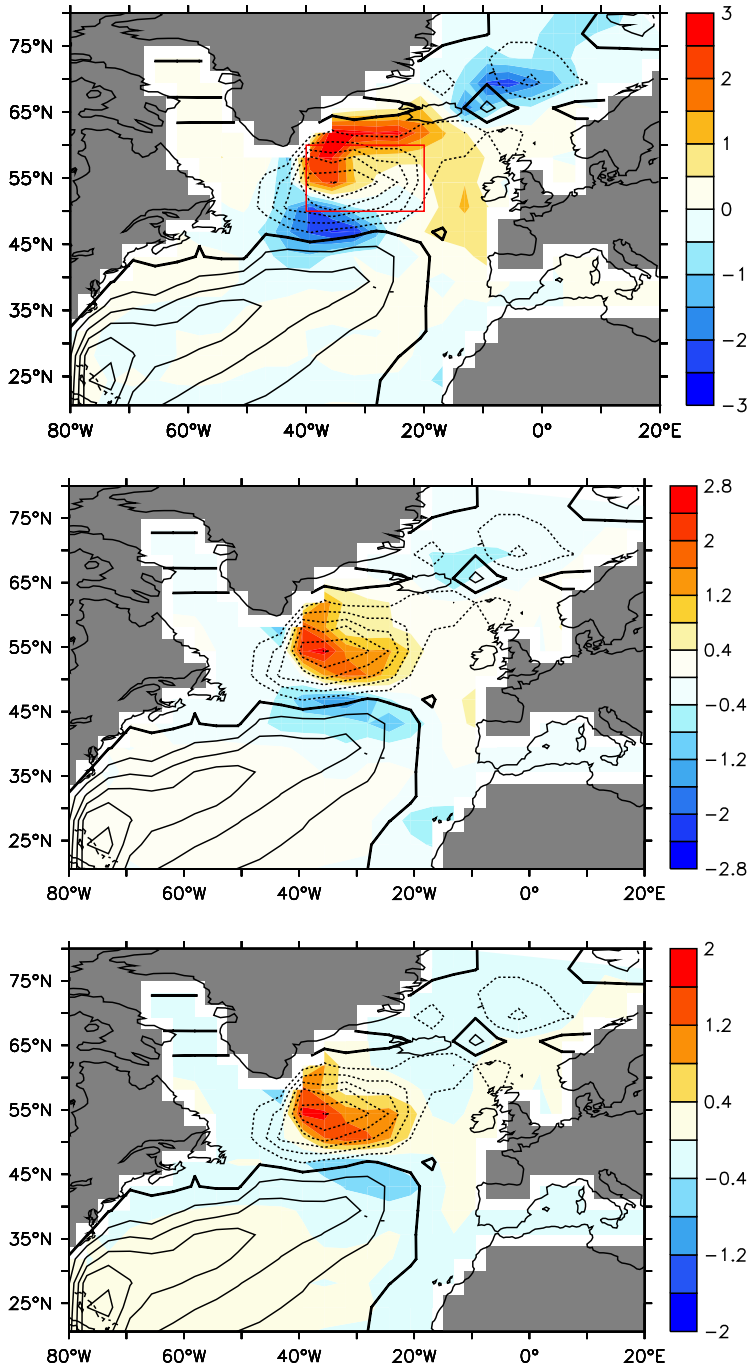

Figure S7: Difference 'after' minus 'before' meltwater pulse, averaged annually and over the upper 75m: temperature (in °C, upper), salinity (in psu, middle), and density (in kg m^{-3}, lower). Steamlines indicate the location of the subpolar gyre after the transition. The region used for averages in figures 2 of the main text and S8 is shown in red.

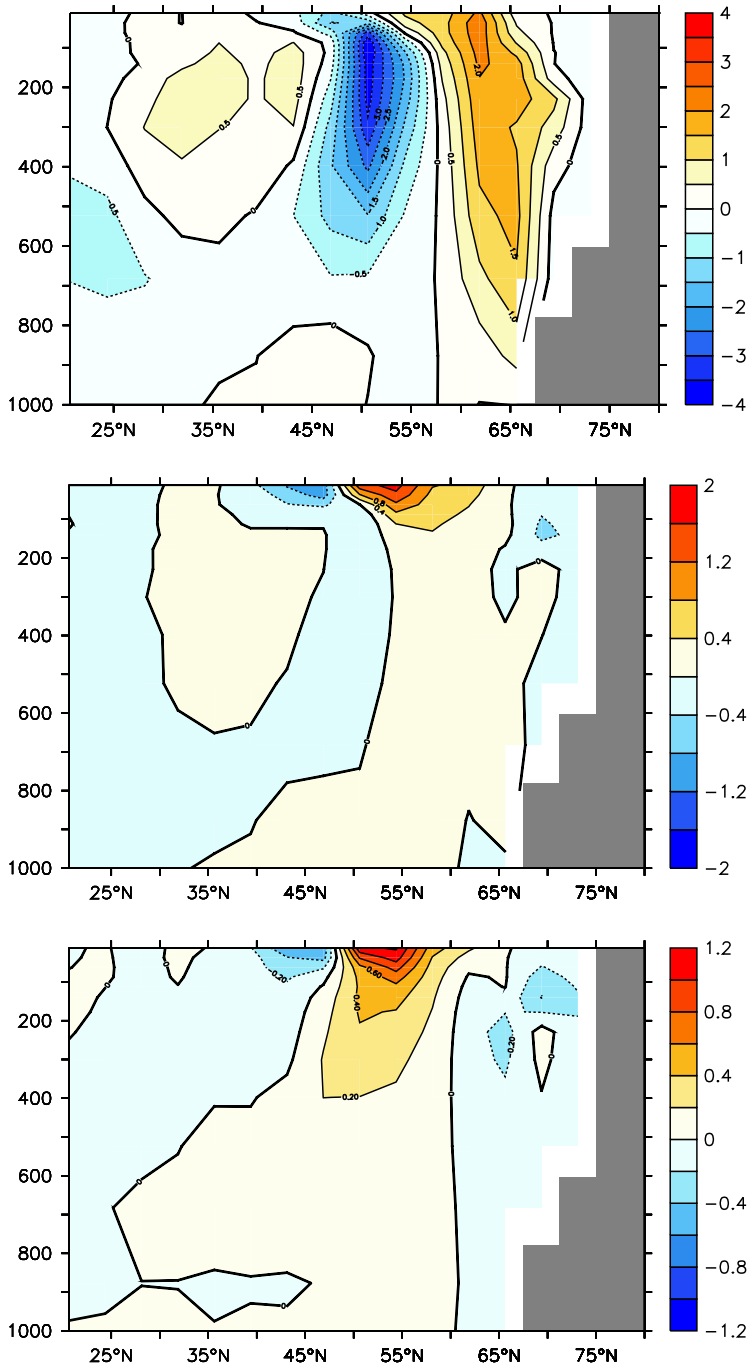

Figure S8: Difference 'after' minus 'before' meltwater pulse, averaged annually and between 40°W and 20°W: temperature (in °C, upper), salinity (in psu, middle), and density (in kg m^{-3}, lower). The largest difference in salinity is seen on the surface due to changes in the advection. In contrast, temperature changes change primarily in subsurface waters because of stronger isopycnal mixing and convection.

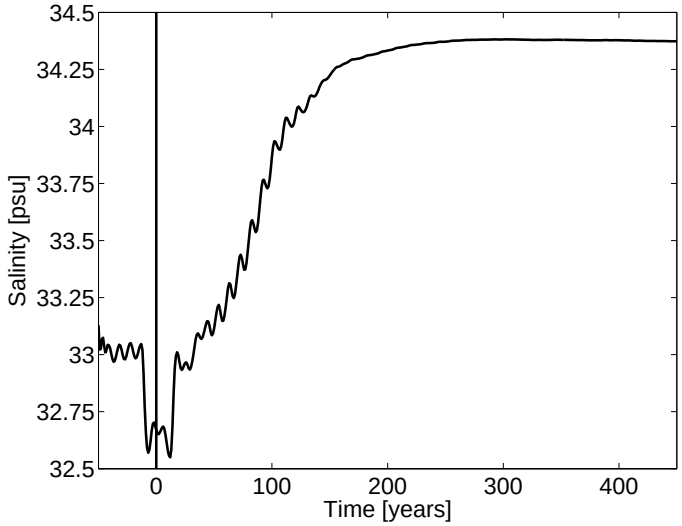

Figure S9: Temporal evolution of annual average sea surface salinity in the center of the subpolar gyre, averaged between 50°N and 60°N and 40°W and 20°W (red rectangle in fig. S7) and filtered with a 25-year running mean. The vertical line indicates the simulated lake Agassiz drainage.

Table S1: List of marine sediment cores used in this study. Magnitude (ΔSST), start of the SPG transition and proxy method are shown where applicable.

Abbreviation in Fig. 1	Full name	ΔSST (°C)	Start (yr BP)	Method	References
HU13	HU90–013–013P	-3	8,200	dinocyst assemblages	*Hillaire-Marcel et al.* (2001) *Solignac et al.* (2004) *de Vernal and Hillaire-Marcel* (2006)
HU21	HU84–030–021TWC&P	-5	8,500	dinocyst assemblages	*de Vernal and Hillaire-Marcel* (2006)
HU94	HU91–045–094P	-5	7,800	dinocyst assemblages	*Hillaire-Marcel et al.* (2001) *Solignac et al.* (2004) *de Vernal and Hillaire-Marcel* (2006)
OCE326 –GGC26	OCE326–GGC26	-3	8,000	alkenones	*Keigwin et al.* (2005) *Sachs* (2007)
LO09-14	LO09-14 LBC/GGC/GC	+2.5	8,000	diatoms	*Andersen et al.* (2004)
ODP984	ODP Site 984	+1.5	8,000	Mg/Ca	*Came et al.* (2007)
MD2251	MD99–2251			sortable silt	*Ellison et al.* (2006)
MD2665	MD03–2665			δ^{13}C & grain size	*Kleiven et al.* (2008)
NEAP4k	NEAP4k			sortable silt	*Hall et al.* (2004)

References

Andersen, C., N. Koc, and M. Moros (2004), A highly unstable Holocene climate in the subpolar North Atlantic: evidence from diatoms, *Quaternary Science Reviews*, *23*, 2155–2166.

Bauer, E., A. Ganopolski, and M. Montoya (2004), Simulation of the cold climate event 8200 years ago by meltwater outburst from Lake Agassiz, *Paleoceanography*, *19*, PA3014.

Born, A., A. Levermann, and J. Mignot (2009), Sensitivity of the Atlantic ocean circulation to a hydraulic overflow parameterisation in a coarse resolution model: Response of the subpolar gyre, *Ocean Modelling*, *27 (3-4)*, 130–142.

Born, A., K. H. Nisancioglu, and P. Braconnot (2010a), Sea ice induced changes in ocean circulation during the Eemian, *Climate Dynamics*, *online*, doi: 10.1007/s00382-009-0709-2.

Born, A., K. H. Nisancioglu, B. Risebrobakken, and A. Levermann (2010b), Late Eemian warming in the Nordic Seas as seen in proxy data and climate models, *Paleoceanography*, *in revision*.

Came, R. E., D. W. Oppo, and J. F. McManus (2007), Amplitude and timing of temperature and salinity variability in the subpolar North Atlantic over the past 10 k.y., *Geology*, *35*, 315–318.

de Vernal, A., and C. Hillaire-Marcel (2006), Provincialism in trends and high frequency changes in the northwest North Atlantic during the Holocene, *Global and Planetary Change*, *54*, 263–290.

Eden, C., and J. Willebrand (2001), Mechanism of Interannual to Decadal Variability of the North Atlantic Circulation, *Journal of Climate*, *14*, 2266–2280.

Ellison, C. R. W., M. R. Chapman, and I. R. Hall (2006), Surface and Deep Ocean Interactions During the Cold Climate Event 8200 Years Ago, *Science*, *312*, 1929–1932.

Fichefet, T., and M. A. M. Maqueda (1997), Sensitivity of a global sea ice model to the treatment of ice thermodynamics and dynamics, *Journal of Geophysical Research*, *102*, 12,609.

Häkkinen, S., and P. B. Rhines (2004), Decline of subpolar North Atlantic circulation during the 1990s, *Science*, *304*, 555–559.

Hall, I. R., G. Bianchi, and J. R. Evans (2004), Centennial to millenial scale Holocene climate-deep water linkage in the North Atlantic, *Quaternary Science Reviews*, *23*, 1529–1536.

Hasumi, H., and N. Suginohara (1999), Effects of locally enhanced vertical diffusivity over rough bathymetry on the world ocean circulation, *Journal of Geophysical Research*, *104*, 23,364–23,374.

Hillaire-Marcel, C., A. de Vernal, A. Bilodeau, and A. J. Weaver (2001), Absence of deep-water formation in the Labrador Sea during the last interglacial period, *Nature*, *410*, 1073–1077.

Hillaire-Marcel, C., A. de Vernal, and D. J. W. Piper (2007), Lake Agassiz Final drainage event in the northwest North Atlantic, *Geophysical Research Letters*, *34*, L15,601.

Hofmann, M., and M. A. M. Maqueda (2006), Performance of a second-order moments advection scheme in an Ocean General Circulation Model, *Journal of Geophysical Research*, *111*, C05,006.

Jongma, J., M. Prange, H. Renssen, and M. Schulz (2007), Amplification of Holocene multicentennial climate forcing by mode transitions in North Atlantic overturning circulation, *Geophysical Research Letters*, *34*, L15,706.

Kalnay, E., and coauthors (1996), The NCEP/NCAR 40-year reanalysis project, *Bull. Amer. Meteor. Soc.*, *77*, 437–471.

Keigwin, L. D., J. P. Sachs, Y. Rosenthal, and E. A. Boyle (2005), The 8200 year B.P. event in the slope water system, western subpolar North Atlantic, *Paleoceanography*, *20*, PA2003.

Kleinen, T., T. J. Osborn, and K. R. Briffa (2009), Sensitivity of climate response to variations in freshwater hosing location, *Ocean Dynamics*, *59(3)*.

Kleiven, H. F., C. Kissel, C. Laj, U. S. Ninnemann, T. O. Richter, and E. Cortijo (2008), Reduced North Atlantic Deep Water Coeval with the Glacial Lake Agassiz Fresh Water Outburst., *Science*, *319*, 60–64.

Ledwell, J. R., E. T. Montgomery, K. L. Polzin, L. C. S. Laurent, R. W. Schmitt, and J. M. Toole (2000), Evidence for enhanced mixing over rough topography in the abyssal ocean, *Nature*, *403*, 179–182.

LeGrande, A. N., and G. A. Schmidt (2008), Ensemble, water isotope-enabled, coupled general circulation modeling insights into the 8.2 ka event, *Paleoceanography*, *23*, PA3207.

LeGrande, A. N., G. A. Schmidt, D. T. Shindell, C. V. Field, R. L. Miller, D. M. Koch, G. Faluvegi, and G. Hoffmann (2006), Consistent simulations of multiple proxy responses to an abrupt climate change event, *Proceedings of the National Academy of Sciences (US)*, *103*, 837–842.

Levermann, A., and A. Born (2007), Bistability of the Atlantic subpolar gyre in a coarse-resolution model, *Geophysical Research Letters*, *34*, L24,605.

Levitus, S. (1982), *Climatological atlas of the world ocean. NOAA Professional Paper, vol 13*, 173 pp. pp., US Dept of Commerce, Washington DC.

Mignot, J., A. Levermann, and A. Griesel (2006), A decomposition of the Atlantic meridional overturning circulation into physical components using its sensitivity to vertical diffusivity., *Journal of Physical Oceanography*, *36*, 636–650.

Montoya, M., and A. Levermann (2008), Surface wind stress threshold for glacial Atlantic overturning, *Geophysical Research Letters*, *35*, L03,608.

Montoya, M., A. Griesel, A. Levermann, J. Mignot, M. Hofmann, A. Ganopolski, and S. Rahmstorf (2005), The Earth System Model of Intermediate Complexity CLIM*BER*-3α. Part I: description and performance for present-day conditions, *Climate Dynamics*, *25*, 237–263.

Montoya, M., A. Born, and A. Levermann (2010), Reversed North Atlantic gyre dynamics in glacial climate, *Climate Dynamics*, *online*, doi:10.1007/s00382-009-0729-y.

Petoukhov, V., A. Ganopolski, V. Brovkin, M. Claussen, A. Eliseev, C. Kubatzki, and S. Rahmstorf (2000), CLIM*BER*-2: a climate system model of intermediate complexity. Part I: model description and performance for present climate, *Climate Dynamics*, *16*, 1.

Prather, M. J. (1986), Numerical advection by conservation of second-order moments, *Journal of Geophysical Research*, *91*, 6671–6681.

Renssen, H., H. Goosse, and T. Fichefet (2005), Contrasting trends in North Atlantic deep-water formation in the Labrador Sea and Nordic Seas during the Holocene, *Geophysical Research Letters*, *32*, L08,711.

Sachs, J. P. (2007), Cooling of Northwest Atlantic slope waters during the Holocene, *Geophysical Research Letters*, *34*, L03,609.

Solignac, S., A. de Vernal, and C. Hillaire-Marcel (2004), Holocene sea-surface conditions in the North Atlantic–contrasted trends and regimes in the western and eastern sectors (Labrador Sea vs. Iceland Basin), *Quaternary Science Reviews*, *23*, 319–334.

Treguier, A. M., S. Theetten, E. P. Chassignet, T. Penduff, R. Smith, L. Talley, J. O. Beismann, and C. Böning (2005), The North Atlantic Subpolar Gyre in Four High-Resolution Models, *Journal of Physical Oceanography*, *35*, 757–774.

Wiersma, A. P., H. Renssen, H. Goosse, and T. Fichefet (2006), Evaluation of different freshwater forcing scenarios for the 8.2 ka BP event in a coupled climate model, *Climate Dynamics*, *27*, 831–849.

Winsor, P., L. Keigwin, S. J. Lentz, and D. C. Chapman (2006), The pathways and impact of fresh water discharge through Hudson Strait 8200 years ago, *Geophysical Research Abstracts*, *8*, 11,007.

Wu, P., and R. A. Wood (2008), Convection induced long term freshening of the subpolar North Atlantic Ocean, *Climate Dynamics*, *31*, 941–956.